

# An Efficient Metasurface-Based Wireless Power Transfer System for Implantable Medical Devices

S. A. Hosseini<sup>1</sup>, M. Yazdi<sup>1\*</sup>

<sup>1</sup>Faculty of Electrical and Computer Engineering, Babol Noshirvani University of Technology, Babol, Iran.  
abolfazlhosseini@stu.nit.ac.ir, yazdi.mohammad@nit.ac.ir

\*Corresponding author

Received: 21/07/2023, Revised: 27/10/2023, Accepted:10/03/2024.

## Abstract

In this paper, by designing a double metasurface, an efficient wireless power transfer system is proposed for implementable medical applications. This system operates at 2.45 GHz in the medical frequency band and consists of two antennas, a transmitter, and a receiver, along with a double metasurface structure embedded between them. A circular patch antenna for the transmitting end and a small loop antenna on the receiving side are designed. To enhance the efficiency of the system, a double metasurface consisting of two arrays of hexagonal ring unit cells is located between the receiver and transmitter antennas. As the receiver antenna is designed for operation in a human body medium, the effects of antenna displacement as well as material uncertainty on the efficiency of total structure are investigated in which reasonable stability concerning these variations is observed. Finally, as this system is aimed to operate in the human body, the safety of this system has also been approved through the calculation of the specific absorption rate (SAR). The proposed wireless power transfer system can overcome the challenges of using implementable medical electronic devices such as battery-replacing surgeries.

## Keywords

Metasurface, Wireless power transfer, Implantable antenna

## 1. Introduction

In recent years, with the advancement of technology, the applications of wireless power transfer (WPT) systems have been widely increased. In particular, WPT systems are promising in the field of implantable medical devices in the human body [1]. Changing the battery in the human body is one of the basic problems that can be overcome using wireless power transfer (WPT) technology for the human clinical environment [2]. Thus, WPT systems have attracted tremendous attention from the scientific community to obviate the problems caused by the use of batteries with limited lifetime in implantable devices [3].

There are various approaches to designing WPT structures such as induction technique [4], magnetic coupling [5], simultaneous transfer of wireless information and power based on lasers [6], and RF wireless power transfer [7]. Among these methods, ones that are based on the radiation of electromagnetic waves provide longer transfer distances along with less sensitivity to the orientation of the antennas. In this regard, a rectifier antenna (rectenna) is a promising solution for efficient wireless power transfer [8]. Since the most important parameter of WPT systems is power efficiency, plenty of researches has been performed to improve the efficiency of WPTs. To this aim, various techniques have been presented such as magnetic resonance coupling based on impedance matching [9], optimization of mixed-resonant circuit structures [10], and employing metamaterial structures [11]. Display quotations of over 40 words, or as needed.

Metasurfaces (MSs) as two-dimensional versions of metamaterials have found many applications, such as cloaking[12], absorbers [13], polarization switching[14], beam steering[15-17], and lenses[18-19]. These applications are consequences of attractive extraordinary electromagnetic features introduced by MSs, which are not found in natural materials. Benefiting from MS characteristics, it is also shown that the efficiency of WPT systems can be enhanced. Furthermore, there are different studies on the improvement of

the efficiency of WPTs using MSs, such as employing multi-mode MS [20], near-field focus reflection analysis[21], and coded MSs [22]. Additionally, by using MSs with spiral MNG unit cells, the efficiency of WPT systems in implantable medical devices has been increased [23-27]. Moreover, by combining an antenna with a MS, it is possible to make a meta-transmitter with the capability of improving the WPT efficiency [24] and also a broadband implantable antenna[25].

In this study, a new MS is proposed to improve the efficiency of the WPT system with application in implantable medical devices. It benefits from high refractive index (HRI) characteristic of MS to improve the system efficiency. The effect of increasing number of MS layers on the efficiency of the structure is also studied. For this purpose, a circular patch antenna is used in the transmitter part (Tx) while a loop antenna with high bandwidth is designed for the receiver part (Rx). Additionally, the effect of possible changes and inconsistencies of the receiver antenna, including as its vertical and horizontal displacements and its rotation on the efficiency of the system is investigated. Moreover, the effects of uncertainty of electrical properties of the human body such as relative permittivity and conductivity coefficients are also analyzed. Finally, considering the importance of human immunity, the specific absorption rate (SAR) of the proposed structure is calculated, which ensures complete immunity. Thus, the proposed system can be a good candidate for increasing efficiency of WPT system with high stability and low SAR.

The remainder of this paper is organized as follows. Section 2 of the paper presents design details of transmitter and receiver antennas to establish a basic wireless power transfer system. The third section is devoted to designing a metasurface for improving the efficiency of the WPT system. Since the proposed structure is designed for working in the human body, a sensitivity analysis is carried out concerning material uncertainty and antenna movement in the fourth section. To ensure health considerations, the sixth section is devoted to the

safety and SAR analysis. Finally, the paper will be concluded in the seventh section.

## 2. Design of basic WPT system

In this section, the basic WPT system for medical applications is designed and its efficiency will be analyzed. The WPT system is composed of at least one transmitter and one receiver antenna which operate in different mediums. The receiving antenna has to be embedded in the human body while the transmitting antenna works in the air medium keeping a definite distance to the human body. Thus, the receiving and transmitting antenna should provide different characteristics which are described in the forthcoming subsections. It is worth noting that the operating frequency for this system is chosen at 2.45 GHz which is an allowed frequency for medical applications.

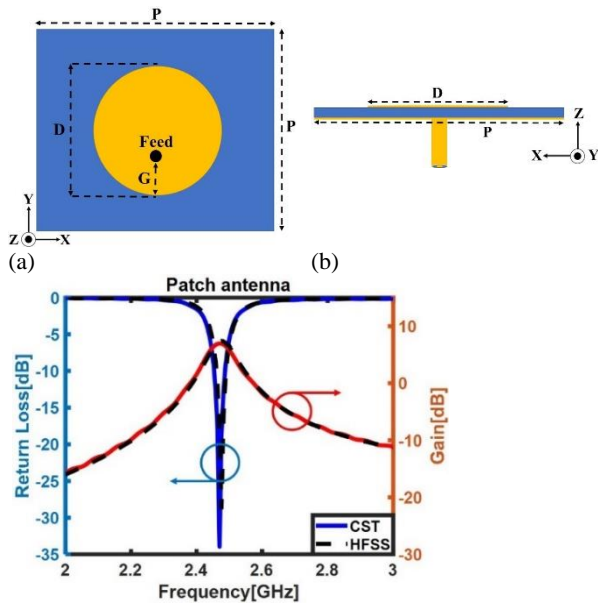


Fig. 1. Schematic of proposed transmitting antenna (a) front view, (b) side view with parameters value as  $P = 80\text{mm}$ ,  $D = 39.6\text{mm}$ ,  $G = 15.2\text{mm}$ , (c) simulated return loss and realized gain of the antenna. the CST results are indicated with solid lines while HFSS results by dashed lines.

### 2.1. Transmitting antenna

The transmitting antenna which operates in the air medium should be a simple, compact, and relatively high-gain antenna. Hence, a circular microstrip patch antenna with a probe-feeding structure has been selected for the transmitting end. Regarding to the feed location, the antenna provides linear y-polarized radiation. The antenna configuration is sketched in Figure 1. (a,b). As shown, it is designed on a Rogers 6002 substrate with a dielectric constant of 2.95 and a loss tangent of 0.0012 with a height of 1.27 mm. To perform numerical full-wave simulations, the commercial full-wave simulator CST Studio Suite [28] has been utilized here. The results also verified with another full-wave simulator, namely ANSYS HFSS simulator [29], and shown with the dashed line in the figures. The antenna parameters are optimized for having good impedance matching and radiation characteristics at 2.45 GHz by the genetic algorithm with population size=50 and crossover=0.8. The optimized parameters are as follows:  $p = 80\text{mm}$ ,  $r = 39.6\text{mm}$ , and  $g = 15.2\text{mm}$ . The return loss of the optimized antenna is shown in Figure 1 (c). As can be seen, the antenna has a return loss lower than -10dB from 2.43 to 2.46 GHz which is desired for the proposed WPT system. Moreover, the antenna has a realized gain of 7.5 dB in the operating frequency range.

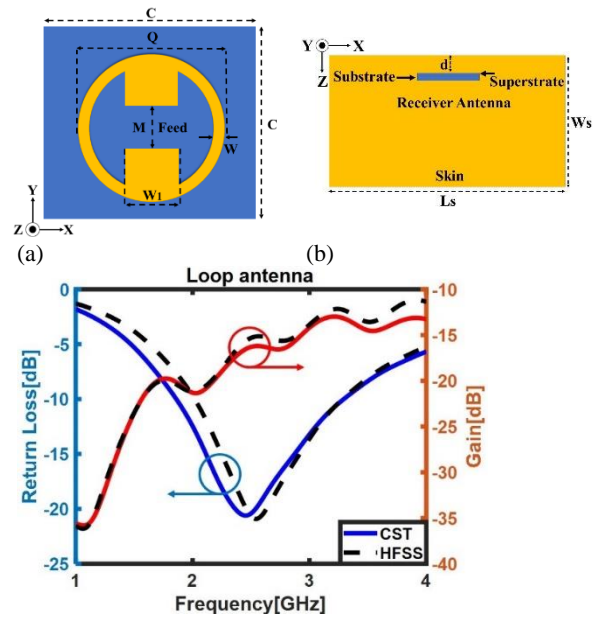


Fig. 2. Schematic of proposed receiving antenna (a) front view, (b) side view and its location in skin medium with parameters value as  $Q = 10\text{mm}$ ,  $C = 12\text{mm}$ ,  $W = 0.5\text{mm}$ ,  $W1 = 4\text{mm}$ ,  $d = m = 3\text{mm}$ ,  $Ls = 80\text{mm}$ ,  $Ws = 30\text{mm}$  (c) simulated return loss and realized gain of the antenna. the CST results are indicated with solid lines while HFSS results by dashed lines.

### 2.2. Receiving implantable antenna

The receiving antenna for the proposed system should be implantable in the human body. Thus, a small antenna structure with a nearly omnidirectional radiation pattern has been designed. The antenna has been mounted on the Rogers 6010 platform, which has a high dielectric constant of  $\epsilon_r = 10.2$ , and a loss tangent of 0.0023 with a thickness of 0.3 mm. In addition, the antenna is masked with a superstrate with similar characteristics to its substrate with 0.1 mm thickness to protect it in the human body environment. To consider the human body effects, the receiving antenna is located in a structure with similar characteristics to the skin at the frequency of 2.45 GHz,  $\epsilon_r = 38$  and  $\sigma = 1.44\text{ S/m}$  equation dimensions of  $80 \times 80 \times 30\text{mm}^3$ . Figure 2 (a,b) shows the schematic of the receiver antenna structure which is located in the human body. The feeding direction of the antenna is designed such that it supports y-polarized linear radiation identical to the transmitter's one. The antenna's parameters are optimized through the genetic algorithm with population size = 50 and crossover = 0.8 to have maximum impedance bandwidth and omnidirectional radiation pattern. The optimized values obtained as:  $q = 10\text{mm}$ ,  $c = 12\text{mm}$ ,  $w = 0.5\text{mm}$ ,  $a = 4\text{mm}$ ,  $m = 3\text{mm}$ . The simulated return loss of the antenna is sketched in Figure 2 (c) which shows a relatively wide impedance bandwidth from 1.6 to 3.7 GHz. Furthermore, the antenna has a nearly omnidirectional pattern with a realized gain of about -17.5 dB which is suited for antennas working in the human body.

### 2.3. Efficiency of basic WPT system

With the designed transmitter and receiver antennas, in this step a basic WPT system from air to the human body is established. The most important parameter in a wireless power transfer (WPT) system is its power transfer efficiency which is defined as the ratio of received power ( $P_r$ ) to transmitted power ( $P_t$ ) Thus, the efficiency of the WPT system can be calculated as:

$$\eta = \frac{P_r}{P_t} = |S_{21}|^2 \quad (1)$$

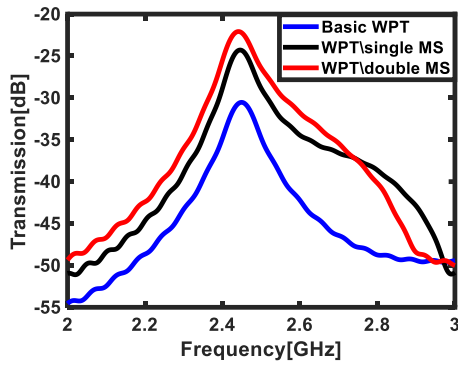


Fig. 3. Simulated transmission (efficiency) of basic WPT system and WPT systems after inserting metasurfaces

The simulated efficiency of the basic WPT system is shown in Figure 3. As shown, the transmitter antenna is placed at a distance of  $d_1 = 100$  mm from the skin edge whereas the receiver antenna has a distance of  $d = 3$  mm from that. Moreover, the antennas are aligned for maximum power transfer. As can be observed,  $|S_{21}| = -30.5$  dB, and the efficiency of the current WPT system is calculated from (1) about 0.09%. The next section is aimed to increase the efficiency by using a metasurface located in the middle of the transmitter and receiver antennas.

### 3. Metasurface Design and Analysis

As mentioned in [31], the efficiency of a WPT system can be increased by using a high refractive index (HRI) Metasurface. Actually, by using an HRI metasurface above the skin layer, the effective aperture of the implantable antenna is enhanced, leading to a significant improvement in power transfer efficiency (PTE). Therefore, an HRI MS can focus the transmitted power wave to the receiver antenna by creating a high refractive index. Here, a hexagonal metasurface is proposed which is printed on both sides of the Rogers 6010 with a dielectric constant of 10.2 and loss tangent of 0.0023. A unit cell of the proposed MS shown in Figure 4 (a,b) is simulated considering periodic boundary conditions in the  $x$  and  $y$  directions. Also, two Floquet ports are applied in the  $z$  direction to obtain the reflectance and transmittance of the total MS structure. Then, using these extracted parameters the effective refractive index ( $n_{eff}$ ), of the MS can be calculated as [32]:

$$n_{eff} = \frac{1}{kh} \cos^{-1} \left[ \frac{1}{2T} (1 - R^2 + T^2) \right] \quad (2)$$

Where  $h$  represents the thickness of the MS and  $k$  is the free space wave number. The proposed unit cell is optimized by the genetic algorithm with population size=50 and crossover =0.8 to provide high refractive index. The extracted effective index is shown in Figure 4 (c) where a high refractive index can be observed. As can be seen, the real part of the refractive index is about 200 showing the HRI nature of the proposed MS at the frequency of interest, 2.45 GHz. Meanwhile, the imaginary part of the refractive index which is related to the loss of the structure is negligible. Thus, the proposed MS could be considered a good candidate for PTE enhancement of the basic WPT system.

As shown in Figure 5 (a), an MS composed of  $4 \times 4$  identical unit cells is placed in the middle of the transmitter and receiver antennas in the human body. The simulated results included in Figure 3 show a -6dB increment in  $S_{21}$  of two antennas compared to the case of the basic WPT system without MS. To attain more enhancement of the efficiency, two  $4 \times 4$  MSs named as double MS with a distance of  $d_3$  have been used, as shown in Figure 5 (b). This structure can be easily fabricated with some electrically transparent spacers between two MSs. To find the best point for the location of the double MSs, a parametric study

is carried out on the two parameters  $d_2$  and  $d_3$  which respectively indicate the distance between the human body and the double MS, and its thickness.

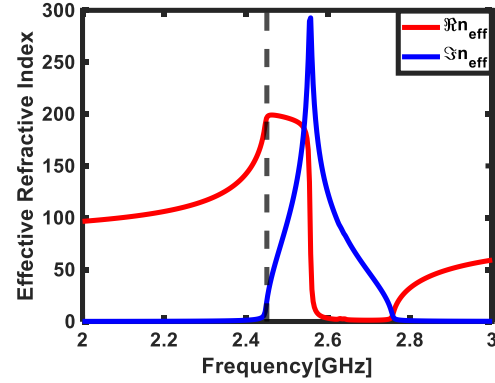
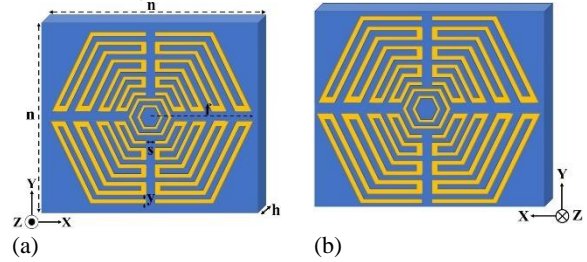


Fig. 4. The schematic of the proposed Unit cell (a) front side, (b) backside, with  $n = 14$ mm,  $f = 6.8$ mm,  $s = 0.4$ mm,  $y = 0.2$ mm,  $h = 0.635$ mm, (c) extracted effective refractive index.

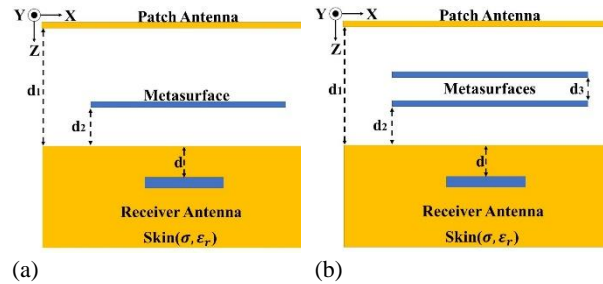


Fig. 5. Improving the efficiency of basic WPT system by inserting MS between Tx and Rx antennas, (a) first scenario with single MS,  $d = 3$ mm,  $d_1 = 100$ mm,  $d_2 = 12$  mm, (b) second scenario with double MS,  $d = 3$ mm,  $d_1 = 100$ mm,  $d_2 = 12$ mm,  $d_3 = 10$ mm.

Table 1. The optimized parameters values of double MS WPT system

$d_2, mm$	$d_3, mm$	$S_{21}, dB$	$\Delta S_{21}, dB$
4	5	-24.5	6
8	5	-23.8	6.7
12	5	-23.5	7
14	5	-23.8	6.7
4	10	-22.3	8.2
8	10	-22.2	8.3
12	10	-22.1	8.4
14	10	-22.3	8.2

The optimized parameters values are tabulated in Table 1, which shows that the  $S_{21}$  of two antennas increases by increasing the distance of the MS from the human body,  $d_2$ . However, going more than  $d_2 = 12$  mm decreases the efficiency which can be explained regarding to the role of the MS as an HRI plate. Furthermore, the maximum efficiency is obtained for  $d_3 = 10$  mm which could be realized by a simple air spacer. The result of the optimized double MS structure in Figure 3 shows an improvement of about 8.4 dB in the  $S_{21}$  of two

antennas compared to the case of basic WPT without any MS. Also, in Figure 6(a), the efficiency improvement graph is presented in which an enhancement from 0.09% to 0.63% is obtained. Besides, Figure 6(b) investigates the effect of MS structure on the input matching of the receiver and transmitter antennas. As can be observed, the MS structure has no significant change in the return loss of the antennas which is a desired characteristic for WPT systems. Up to now, a MS that is capable of increasing WPT efficiency is designed and optimized. In the next section, a sensitivity analysis of this system for different cases will be performed. To better illustrate the role of the MS in increasing WPT efficiency, a WPT system can be modeled by a two-port system. Having the Z-parameters of the WPT system in hand, its efficiency can be obtained as [33]:

$$\eta = \frac{P_{out}}{P_{in}} = \frac{R_{load} |Z_{21}|^2 \Re\{Z_{in}\}}{|Z_{22} + R_{load}|^2 |Z_{in}|^2} \quad (3)$$

Where  $R_{Load}$  is the load resistance of the receiving end. Moreover,  $Z_{in}$  stands for the input impedance of the transmitting end calculated as:

$$Z_{in} = Z_{11} - \frac{Z_{12}Z_{21}}{(Z_{22} + R_{load})} \quad (4)$$

Regarding to above formulas, the efficiency of a WPT system is a function of its Z-parameters as well as load impedance. Since the load impedance is usually set to  $R_{load} = 50 \Omega$ , here the focus would be only on the Z-parameters. The Z-parameters of the WPT system with and without using double MS have been calculated and the results are depicted in Fig. 7. Figure 7(a,b) demonstrates that embedding MS in the WPT system does not change the  $Z_{11}$  and  $Z_{22}$  parameters. This is due to the enough distance between MS and antennas, which leads to minimum coupling on the antennas. Thus, the effect of adding MS mainly appears in  $Z_{21}$  as suggested by Fig. 7(c). As a result, based on equation (3) increasing  $Z_{21}$  improves the total efficiency of the WPT system. Therefore, the efficiency of the WPT system with and without double MS is calculated and depicted in Fig. 7(d). As can be observed, the results are similar to Fig. 6(a), which shows the theoretical calculation and simulation results of efficiencies are in good agreement.

#### 4. Sensitivity Analysis of Improved WPT System

After designing the MS for increasing WPT efficiency, it is required to perform a sensitivity analysis of the total structure concerning either spatial displacement or material parameters uncertainty. In this section, firstly the effect of changes in spatial parameters will be investigated, and then the changes in material parameters will be investigated.

##### 4.1. Spatial displacement

There are several spatial parameters which are important to be studied for a system working in a human body environment. Regarding Figure 8, the effects of four parameters are considered here including  $d_t$ ,  $d$ ,  $dx$ ,  $\theta$ . Firstly, the effect of distance between transmitter and receiver antennas,  $d_t$ , on the  $S_{21}$  of two antennas will be investigated.

As expressed in Table 2, transmission parameter,  $S_{21}$ , decreases by increasing the distance between two antennas which is due to the attenuation of free space loss. Nevertheless, the role of the MS in increasing  $S_{21}$  is reserved in all values of  $d_t$ . As can be seen, there are at least 8.4 dB enhancement in  $S_{21}$  in all cases, which verifies the effectivity of the MS structure in efficiency improvement.

Another important issue in the WPT system for implants is the displacement of the receiver antenna in the human body. Here, the effect of possible displacement as well as rotation of the receiver antenna on the performance of the proposed system should be studied. At first, the receiver antenna is allowed to move vertically in the human body with amount of  $d$  from the surface of the skin, as illustrated in Figure 8. The values of the  $S_{21}$  in different locations of the receiver antenna are calculated and shown in Fig. 9(a). As can be seen, by moving the receiver antenna far from the surface of the skin, the amount of received power is decreased which is a natural consequence of free space loss. Nevertheless, there is still efficiency improvement concerning the case of the WPT system without using any MS. Next, will allow the receiver antenna in the human body to move horizontally with an amount of  $dx$  from the center, as shown in Fig. 8, where the corresponding results are shown in Fig. 9(b). As can be realized, increasing  $dx$  reduces the value of  $S_{21}$  which is an expected result. Indeed, this is due to the displacement of the receiver antenna from the focus center of MSs. However, this can be easily modified by using an adjustable MS structure to dynamically focus on the new location of the receiver antenna. Again, an increase with respect to the case of without MSs can be still observed in all cases of Fig. 9(b).

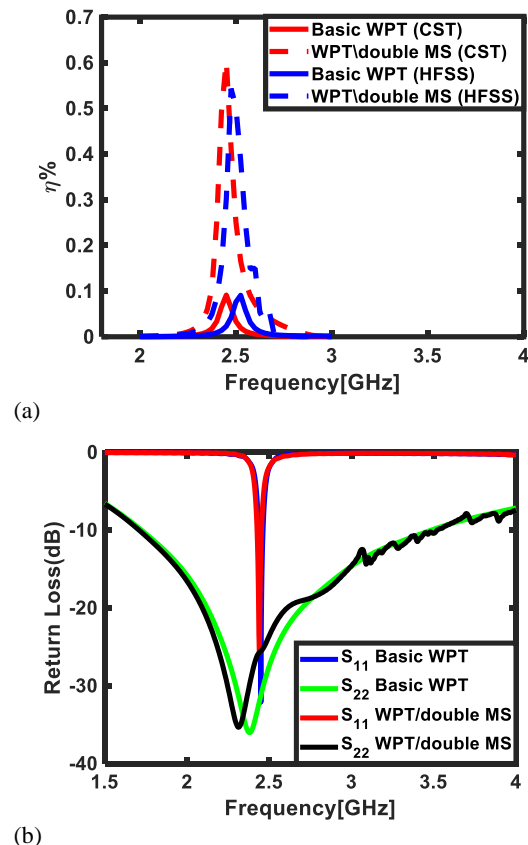


Fig. 6. The effect of adding double MS on the basic WPT system, (a) efficiency increases, the CST results are indicated with solid lines while HFSS results by dashed lines (b) the return losses of the antennas remain unchanged.

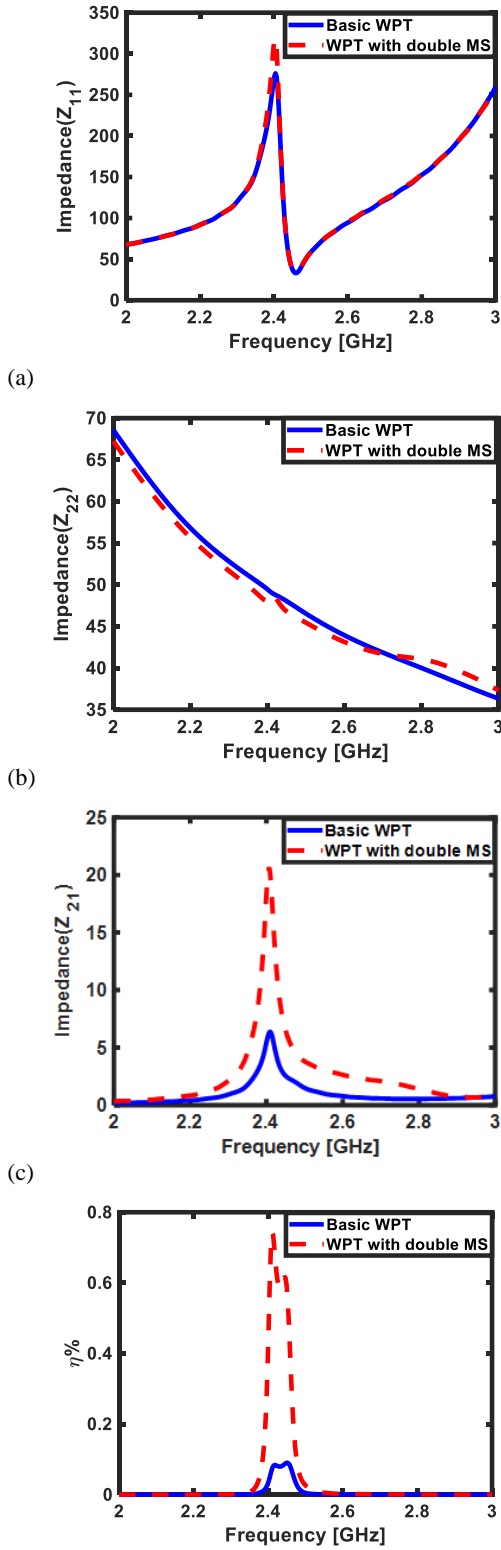


Fig. 7. Comparison of Z-parameters of basic WPT system and WPT system with double MS. (a)  $Z_{11}$ , (b)  $Z_{22}$ , (c)  $Z_{21}$ , (d) efficiency.

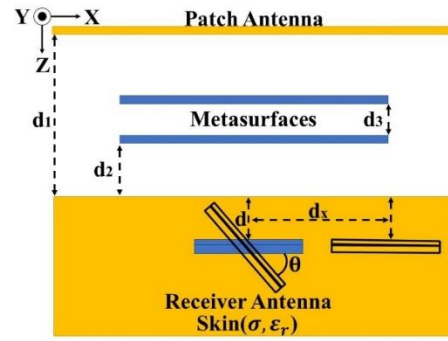


Fig. 8. Scheme of sensitivity analysis scenario with respect to spatial displacement including three parameters' effects  $d_1$ ,  $d$ ,  $dx$ ,  $\theta$ .

Table 2. The effect of increasing distance between transmitter and receiver ( $d_1$ ) on the efficiency of the WPT system ( $S_{21}$ )

$d_1$ [mm]	$S_{21}$ [dB]	
	Without MS	With MS
100	-30.52	-22.1
110	-31.04	-23.10
120	-32	-24.00
130	-32.5	-24.74
140	-32.88	-25.32
150	-33.63	-25.61

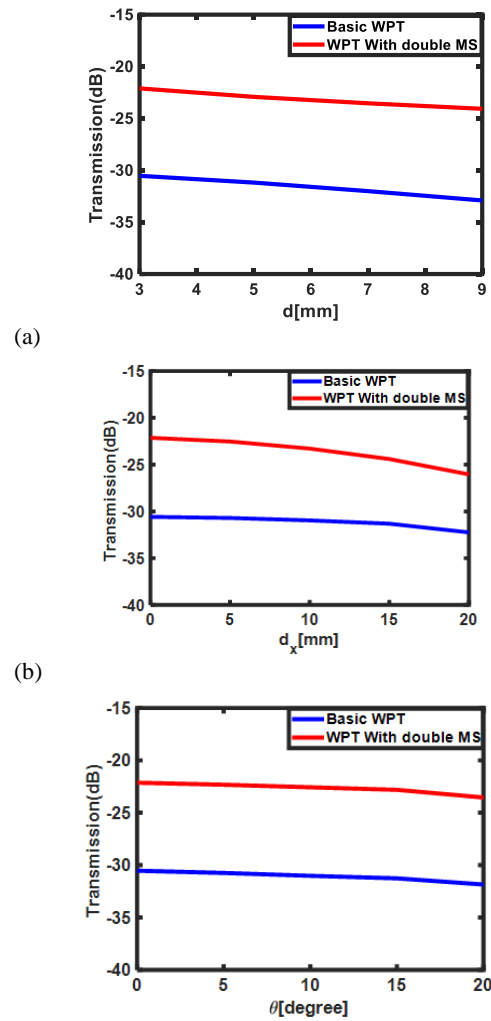
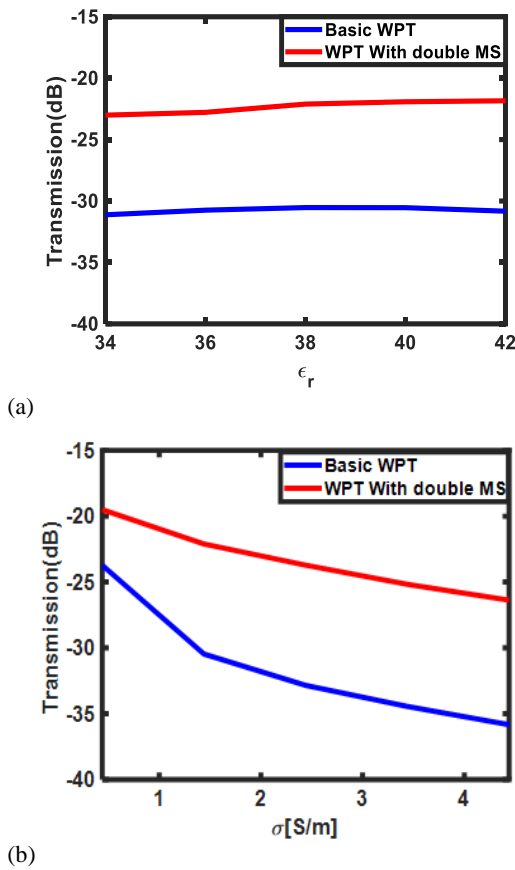


Fig. 9. The effects of spatial displacement on the efficiency of the WPT system without and With MSs: (a)  $d$ , (b)  $dx$ , (c)  $\theta$  as indicated in Fig. 8.

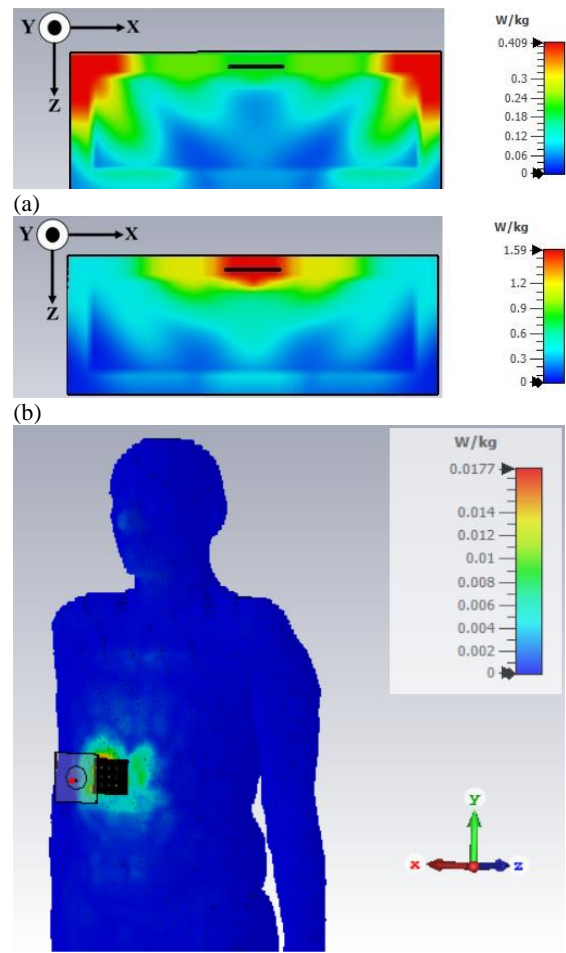


(a) (b)  
**Fig. 10. Investigating the effect of environmental parameters on the transmission of the WPT systems. (a) Permittivity ( $\epsilon_r$ ) (b) conductivity ( $\sigma$ ) of skin medium.**

Lastly, the effect of rotation of the receiver antenna, as a common occurrence in the real human body, is studied. The schematic of the considered scenario is depicted in Fig. 8 where the antenna is allowed to rotate around its center by the angle of  $\theta$ . The rotation angle is varied from 0 to 20 degrees, and the corresponding results are shown in Fig. 9(c). As can be observed, the WPT efficiency is decreased by increasing the rotation angle due to the misalignment between the transmitter MS and receiver antenna. However, again there is a good amount of improvement compared to the basic WPT case.

#### 4.2. Effect of environment characteristics

A practical WPT system should also consider the effect of uncertainties in the amounts of permittivity ( $\epsilon_r$ ) as well as conductivity ( $\sigma$ ) of the human body. In this section, a sensitivity analysis of WPT performance is performed on the conductivity and permittivity changes. In the previous sections  $\epsilon_r = 38$  and  $\sigma = 1.44$  S/m are used for the human body. Here, the dependence of  $S_{21}$  on variations of permittivity is depicted in Fig. 10(a) where the conductivity is set to  $\sigma = 1.44$  S/m. Moreover, Fig. 10(b) shows the effect of different conductivity values on  $S_{21}$  where the permittivity is fixed at  $\epsilon_r = 38$ . Although there is no significant change in  $S_{21}$  with increasing permittivity, it decreases with increasing conductivity. The latter effect is due to the increasing loss which is a direct consequence of increasing conductivity.



(c)  
**Fig. 11. Distribution of power loss density for 1g of the human body at 2.45 GHz frequency. (a) Basic WPT system (b) WPT with double MS, the receiver antenna can be located in the middle top of the pictures (c) calculation of SAR value near the human body phantom.**

### 5. Safety and SAR analysis

Since WPT systems interact directly with the human body, safety analysis is a necessary examination to ensure that they have no bad health impacts. To confirm the safety considerations of a WPT system working around the human body, the specific absorption rate (SAR) is usually calculated, which is evaluated from the energy

stored in the human body. According to the IEEE C95.3 standard [34], the SAR value of a WPT system should not exceed 1.6 W/kg to preserve patient safety. In this study, the SAR investigation is performed on the proposed WPT system for a 1g average of the human body. Furthermore, the results are examined according to the power changes in the transmitter to find the maximum input power before that meets SAR considerations. The changes of SAR are compared in two cases basic WPT and WPT with double MS. From the results of Table 3, it is obvious that considering 1W of power in the transmitter SAR results in 2.05W/kg SAR for basic WPT. However, using double MS in the WPT system increases SAR to 7.94W/kg which is due to the high focus of the wave energy to the receiver location. This is illustrated in Figure 11 where a high concentration of power loss around the receiver antenna after embedding the double MS could be distinguished. Obviously, the SAR value could be reduced by decreasing the input power. Finally, the values of SAR are calculated for different input powers of the WPT system with double MSs and tabulated in Table 3. It is shown that the input power of the transmitter antenna, in this case,

should be kept under 0.2 W to ensure the SAR value would be in the specified standard range. This illustrates the advantage of using MS in WPT system, which reduces the input power from more than 0.5 W in the case of WPT without MS, to 0.2 W in the case of WPT with MS, while keeping the output SAR level at 1.6 W/kg. It should be noticed that in the implementable WPT systems the allowed SAR density is limited due to the safety standards. However, WPT systems with higher efficiencies need less input power to reach this limitation. Furthermore, a human body phantom is used to calculate the SAR value as shown in Fig. 11(c). As can be observed, the proposed double MS succeeded in focusing transmitting power to the receiver location, which prevents harming other parts of the body.

**Table 3. Calculated 1 g average SAR (W/kg)**

Input power (W)	Without MSs	With MSs
1.00	2.05	7.94
0.50	1.02	3.97
0.25	0.51	1.98
0.20	0.28	1.59

In Table 4, the results of this paper are compared with other reported works on metasurface-based WPT systems. All the references are designed for implementable applications working at the ISM frequency band. As shown, all of them use relatively high-gain, low-profile, narrowband microstrip antennas for transmitting end, while low-gain, small antennas with wider bandwidth are used for receiving end. The transmission improvement made by the metasurface with respect to the case without the metasurface is also compared for all references. Although some references achieve higher transmission improvement than this paper, their transfer distance is much lower than what is presented here. Consequently, the proposed design can be regarded as a good candidate for WPT charging of implementable WPT sensors.

**Table 4. Comparisons among WPT systems**

Ref	Antenna Gain (dB)		Bandwidth (%)		Improvement $\Delta S_{21}$ (dB)	Transfer Distance (mm)
	Tx	Rx	Tx	Rx		
[25]	N.M*	-32	1.5	139	11	50
[26]	7.5	1.9	0.5	4	5.62	60
[27]	2	-23	23	9	8	14
[31]	7.8	-14	2	45.2	6	53
This work	7.5	-18	1.3	80	8.4	100

\*N.M. means not mentioned in the reference.

## 6. Conclusion

In this study, a double metasurface has been employed to improve the efficiency of the wireless power transfer (WPT) system. The obtained results show that using double MS enhances power transmission and efficiency percentage respectively about 8.4 dB and 600%. Also, a comprehensive sensitivity analysis is performed including the effect of displacement and rotation of the receiving antenna and uncertainty in the human body parameters where an acceptable robustness is observed. Furthermore, the performance of the proposed system is investigated through a theoretical analysis based on a two-port network model where the theoretical predictions are well matched with simulation results. Finally, a safety analysis is carried out which shows that the calculated

SAR value meets its standard range if the input power of the WPT system does not exceed 0.2 W. The overall results show that the designed system is suitable for improving the efficiency and safety of the WPT system. The proposed WPT system is a good candidate for implementable medical electronic devices.

## 7. Acknowledgments

The authors acknowledge the funding support of Babol Noshirvani University of Technology through Grant program No. BNUT/391025/1402.

## 8. References:

- [1] Y. Zhou, C. Liu, and Y. Huang, "Wireless power transfer (WPT) for implanted medical application: A review", *Energies*, vol. 13, no. 11, pp. 2837, 2020.
- [2] C. Xiao, D. Cheng, and K. Wei, "An LCC-C compensated wireless charging system for implantable cardiac pacemakers: Theory, experiment, and safety evaluation", *IEEE Transactions on Power Electronics*, vol. 33, no. 6, pp. 4894-4905, 2017.
- [3] K. Agarwal, R. Jegadeesan, Y. Guo, N. V. Thakor "Wireless power transfer (WPT) strategies for implantable bioelectronics", *IEEE Reviews in Biomedical Engineering*, vol. 10, pp. 136-161, 2017.
- [4] M.R. Usikalu1, S.A. Adewole1, J.A. Achuka1, T.A. Adagunodo1, T.J. Abodunrin1 and L.N. Obafemi. "Investigation into wireless power transfer (WPT) in the near field using induction technique", in *Journal of Physics, Conference Series*, vol. 1299, no. 1, pp. 012047, 2019.
- [5] M. Wang, L. Ren, Y. Shi, W. Liu, H. R. Wang, "Analysis of a nonlinear magnetic Coupling Wireless power transfer (WPT) system", *Progress In Electromagnetics Research C*, vol. 110, pp. 15-26, 2021.
- [6] Y. Wang, C. Zhao, and L. Zhang, "Adaptive High-Power Laser-Based Simultaneous Wireless Information and Power Transfer System With Current-Fed Boost MPPT Converter". *IEEE Photonics Journal*, vol. 13, no. 4, pp. 1-11, 2021.
- [7] C.M. Song, S. Trinh-Van, S.H. Yi, J. Bae, Y. Yang, K.Y. Lee, K.C. Hwang, "Analysis of received power in RF wireless power transfer (WPT) system with array antennas", *IEEE Access*, vol. 9, pp. 76315-76324, 2021.
- [8] B.J. DeLong, A. Kiourti, J.L. Volakis, "A radiating near-field patch rectenna for wireless power transfer (WPT) to medical implants at 2.4 GHz", *IEEE Journal of Electromagnetics, RF, and Microwaves in Medicine and Biology*, vol. 2, no. 1, p. 64-69, 2018.
- [9] T.C. Beh, T. Imura, M. Kato, Y. Hori, "Basic study of improving efficiency of wireless power transfer (WPT) via magnetic resonance coupling based on impedance matching", *IEEE International Symposium on Industrial Electronics*. pp. 2011-2016, 2010.
- [10] L. Chen, S. Liu; Y.C. Zhou; T.J Cui, "An optimizable circuit structure for high-efficiency wireless power transfer", *IEEE Transactions on Industrial Electronics*, vol. 60, no. 1, pp. 339-349, 2011.
- [11] B. Wang, K.H. Teo, T. Nishino, W. Yerazunis, J. Barnwell, J. Zhang, "Experiments on wireless power transfer (WPT) with metamaterials", *Applied Physics Letters*, vol. 98, no. 25, pp. 254101, 2011.
- [12] Y. Yang, L. Jing, B. Zheng, R. Hao, W. Yin, E. Li, C.M. Soukoulis, H. Chen, "Full-polarization 3D metasurface cloak with preserved amplitude and phase", *Advanced Materials*, vol. 28, no. 32, pp. 6866-6871, 2016.
- [13] Y. Cheng, F. Chen, H. Luo, "Triple-band perfect light absorber based on hybrid metasurface for sensing application", *Nanoscale research letters*, vol. 15, no. 1, pp. 1-10, 2020.
- [14] J.B. Mueller, N.A. Rubin, R.C. Devlin, B. Grover, F. Capasso, "Metasurface polarization optics: independent phase

- control of arbitrary orthogonal states of polarization”, *Physical Review Letters*, vol. 118, no. 11, pp. 113901, 2017.
- [15] S.E. Hosseinienejad, K. Rouhi, M. Neshat, A.C. Aparicio, S. Abadal, E. Alarcón, “Digital metasurface based on graphene: An application to beam steering in terahertz plasmonic antennas”. *IEEE Transactions on Nanotechnology*, vol. 18, pp. 734-746, 2019.
- [16] B. R. Rezvan, M. Yazdi, S.E. Hosseinienejad, “A 2-bit programmable metasurface for dynamic beam steering applications”, *Tabriz Journal of Electrical Engineering*, vol. 51, no. 2, pp. 277-284, 2021.
- [17] R. Asgharian, B. Zakeri, M. Yazdi, S. Samadi “Design of Steerable Passive Reflect array Using Non-uniform Elements for main beam and Side Lobe Level improvement”, *Tabriz Journal of Electrical Engineering*, vol. 49, no. 3, pp. 985-993, 2019.
- [18] Z. Zhang, D. Wen, C. Zhang, M. Chen, W. Wang, S. Chen, and, X. Chen, “Multifunctional light sword metasurface lens”, *ACS Photonics*, vol. 5, no. 5, pp. 1794-1799, 2018.
- [19] M. Bozorgi, and, M. Rafaei-Booket, “Reconfigurable planar metasurface lens using TiO<sub>2</sub>: design and simulation”, *Tabriz Journal of Electrical Engineering*, vol. 52, no. 4, pp. 229-237, 2022.
- [20] X. Jiang, R.K. Pokharel, A. Barakat, K. Yoshitomi, “A multimode metamaterial for a compact and robust dual-band wireless power transfer (WPT) system”, *Scientific Reports*, vol. 11, no. 1, pp. 1-10, 2021.
- [21] P. Zhang, L. Li, X. Zhang, H. Liu, Y. Shi, “Design, measurement, and analysis of near-field focusing reflective metasurface for dual-polarization and multi-focus wireless power transfer”, *IEEE Access*, vol. 7, pp. 110387-110399, 2019.
- [22] N.M. Tran, M.M. Amri, J.H. Park, S.II. Hwang, D.I. Kim, K.W. Choi, “A novel coding metasurface for wireless power transfer (WPT) applications”. *Energies*, vol. 12, no. 23, pp. 4488, 2019.
- [23] L. Li, H. Liu, H. Zhang, and W. Xue, “Efficient wireless power transfer (WPT) system integrating with metasurface for biological applications”, *IEEE Transactions on Industrial Electronics*, vol. 65, no. 4, pp. 3230-3239, 2017.
- [24] R.K. Pokharel, A. Barakat, S. Alshhawy, K. Yoshitomi, C. Sarris, Wireless power transfer (WPT) system rigid to tissue characteristics using metamaterial inspired geometry for biomedical implant applications. *Scientific Reports*, vol. 11, no. 1, pp. 1-10, 2021.
- [25] M. Wang, H. Liu, P. Zhang, X. Zhang, H. Yang, G. Zhou, L. Li, “Broadband implantable antenna for wireless power transfer (WPT) in cardiac pacemaker applications”, *IEEE Journal of Electromagnetics, RF and Microwaves in Medicine and Biology*, vol. 5, no 1, pp. 2-8, 2020.
- [26] T. Shaw, G. Samanta, D. Mitra, B. Mandal, and, R. Augustine, “Design of metamaterial based efficient wireless power transfer system utilizing antenna topology for wearable devices”. *Sensors*, vol. 21, no. 10, 3448, (2021).
- [27] I. A. Shah, M. Zada, S. A. A. Shah, A. Basir, and H. Yoo, “Flexible metasurface-coupled efficient wireless power transfer system for implantable devices”, *IEEE Transactions on Microwave Theory and Techniques*. 2023.
- [28] <http://www.cst.com/products/cstmws>.
- [29] <http://www.aonesoft.net/ansys/hfss.html>.
- [30] Z. J. Yang, S. Q. Xiao, L. Zhu, B. Z. Wang, H. L. Tu, A circularly polarized implantable antenna for 2.4-GHz ISM band biomedical applications. *IEEE Antennas and Wireless Propagation Letters*, vol. 16, pp. 2554-2557, 2017.
- [31] T. Shaw, D. Mitra, “Metasurface-based radiative near-field wireless power transfer (WPT) system for implantable medical devices”. *IET Microwaves, Antennas & Propagation*, vol. 13, no. 12, pp. 1974-1982, 2019.
- [32] D.R. Smith, D.C. Vier, Th. Koschny, and C.M. Soukoulis, “Electromagnetic parameter retrieval from inhomogeneous metamaterials”, *Physical Review E*, vol. 71, no. 3, pp. 036617, 2005.
- [33] G. Gonzalez, “Analysis and design microwave transistor amplifiers”, 1997.
- [34] IEEE Recommended Practice for Measurements and Computations of Electric, Magnetic, and Electromagnetic Fields with Respect to Human Exposure to Such Fields, 0 Hz to 300 GHz,” in IEEE Std C95.3-2021 (Revision of IEEE Std C95.3-2002 and IEEE Std C95.3.1-2010), vol., no., pp.1-240, 2021.